

Chapter 3

Electrochemical Solar Cells Based on Pigments

Constantin Turta, Gheorghe Duca, Ion Marin and Dumitru Sirbu

Abstract The intensity of solar radiation at the outer edge of the atmosphere (global illumination on the ground) when the Earth is the average distance from the Sun, is called the solar constant, whose value is $1.37 \cdot 10^6$ ergs/s/cm² ($1.37 \cdot 10^3$ W/m²) or about 2 cal/min/cm² [1]. As a result the Earth receives a total $1.56 \cdot 1,018$ $1.2 \cdot 1,017$ W or kWh/year. In turn burn energy obtained from 1 kg of hydrogen is 39.4 kWh. So the solar energy which comes to Earth is equivalent to $3.9 \cdot 1,016$ kg H₂. During the day-middle solar cell with an efficiency of 10 % produces electrical power 100 W/m². Simple calculations show that the annual European solar surface could give 80 kW/m². This quantity is equivalent to 2 kg H₂ showing that total energy requirements for world could be met to cover only 0.13 % of Earth's surface with solar panels by 10 % efficiency.

Keywords Solar cells · Photoelectrochemistry · Solar energy · Pigments

The main objective of photoelectrochemistry is to produce hydrogen from water photolysis. Electrochemical reaction of water decomposition requires a potential difference $\Delta V = 1.23$ V which is equivalent to three photovoltaic solar cells.

At the moment there are known eight types of solar cells [2], photovoltaic cells:

- (1) silicon cells [(c-Si, monocrystalline, maximum efficiency over 20 %) (mc-Si, polycrystalline, maximum efficiency over 16 %) (a-Si, amorphous thin layer yield 5–7 %)];
- (2) Semiconductor-based elements of group III–V [GaAs (GaInP/GaAs, GaAs/Ge, cosmic space, yield 15–30 %)];

C. Turta (✉) · I. Marin · D. Sirbu
Institute of Chemistry, Academy of Sciences of Moldova, 3 Academiei Str., Chisinau,
Republic of Moldova
e-mail: turtaclba@yahoo.com

G. Duca
Academy of Sciences of Moldova, 1 Stefan cel Mare Ave., Chisinau, Republic of Moldova

Table 3.1 Regional variation of the average cost of new generating resources, 2016 [3]

Plant type	Range for total system levelized costs (2009 \$/MWh)		
	Minimum	Average	Maximum
Conventional coal	85.5	94.8	110.8
Advanced coal	100.7	109.4	122.1
Advanced coal with CCS	126.3	136.2	154.5
Natural gas-fired			
Conventional combined cycle	60.0	66.1	74.1
Advanced combined cycle	56.9	63.1	70.5
Advanced CC with CCS	80.8	89.3	104.0
Conventional combustion turbine	99.2	124.5	144.2
Advanced combustion turbine	87.1	103.5	118.2
Advanced nuclear	109.7	113.9	121.4
Wind	81.9	97.0	115.0
Wind-offshore	186.7	243.2	349.4
Solar PV	158.7	210.7	323.9
Solar thermal	191.7	311.8	641.6
Geothermal	91.8	101.7	115.7
Biomass	99.5	112.5	133.4
Hydro	58.5	86.4	121.4

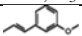
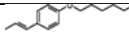
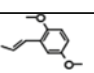
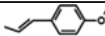


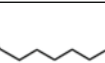
- (3) Semiconductor-based elements of group II–VI (CdTe, yield: Lab.—16 %, in practice—10 %);
- (4) Cells CIS, CIGS [(CuIn(Se)₂), (CuInS₂), (CuInGa (SeO), maximum yield 42 %];
- (5) Solar cells based on organic compounds;
- (6) Cells based on pigments (Grätzel' cells);
- (7) Cells with semiconductor electrolyte (CuO/NaCl);
- (8) Cells based on polymers (in research state).

In Tables 3.1 and 3.2 the prices of one kWh depending on the nature of the source of energy are shown.

Notice that the use of solar energy is currently more expensive than other energy sources.

AM 1.5 size indicates weakening global sunlight at the Earth's surface depending on latitude because browsing a large air masses proportional to the latitude (in this case the 50° latitude is considered). This corresponds to Central European summer conditions—from Northern Italy to central Sweden.

Table 3.2 Absorption coefficients/ $10^3 \text{ M}^{-1} \text{ cm}^{-1}$, efficiency and substituents R_i of Dyes [30]

Dye	Absorption coefficient $10^3 \text{ M}^{-1} \text{ cm}^{-1}$	Efficiency (%)	Radicals
N3	14.2 (534 nm)(ethanol)	10.0	$R_1=R_2=R_3=R_4=H$
N712	---	8.2	$R_1=R_2=R_3=R_4=TBA$
N719	13.6 (535 nm)	11.2	$R_1=R_2=TBA$; $R_3=R_4=H$
Z910	16.9 (543 nm) (acetonitrile)	10.2	$R_1=R_2=$ 
K19	18.2 (543nm) (acetonitrile- <i>t</i> -butylalcohol 1:1)	7.0	$R_1=R_2=$ 
N945	18.9 (550 nm) (acetonitrile- <i>t</i> -butylalcohol 1:1)	10.8	$R_1=R_2=$ 
K73	18.0 (545 nm)	9.0	$R_1=R_2=$ 
N621	---	9.6	$R_1=R_2=$ 
Z907	11.1 (525 nm)	7.3	$R_1=R_2=$ 
Z955	8.0 (519 nm)	8.0	
HRS-1	18.7 (542 nm) (ethanol)	9.5	$R_1=R_2=$ 
Black dye	(610 nm)	10.8	

3.1 Electrochemical Solar Cells Based on Pigments

This cell type is also known as Grätzel cells. Unlike silicon/semiconductor cells, Grätzel cells' power is obtained by using a light-absorbing pigment on titanium oxide semiconductor [4, 5]. The third component of the cell is the electrolyte [5].

As photoanode other different semiconductors can be used: WO_3 , CuI etc. As pigments in principle the rarely metal ruthenium complexes with bipyridyl derivatives as ligands are used, but for demonstration purposes other organic pigments, for instance, chlorophyll or anthocyanins (from berries), which are characterized by a very low lifetime can be used. The operation of this cells type is shown in Fig. 3.1.

At photo-excitation of the pigment molecules absorbed on the surface of n-type/ (p-type) semiconductor it is possible to inject electrons (holes) in the conductor (the valence) band forming a cation (anion) [8–12]. This phenomenon is known as sensitization and has been used successfully in the development of photoelectrochemical pigment-sensitized cells—Dye-sensitized (DS) photoelectrochemical cells (PECS) [13–15].

Our group is working in synthesis of new complexes as photosensitizers for this type of solar cells.

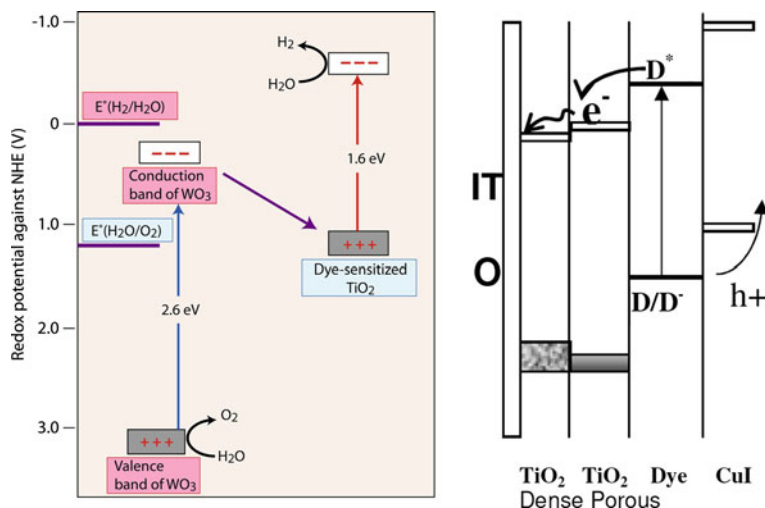


Fig. 3.1 Scheme of photolysis tandem system (left) [6] and TiO_2 band positions, the ground and excited states of ruthenium complex with bipyridyl (right) [7], illustrating the mechanism of charge separation

3.2 Complexes of Ruthenium with Bipyridine and Terpyridine

3.2.1 $Ru(bpy)$ -Complexes

The achieved progress in optimization of dyes used in dye sensitizer solar cells (DSSC) was performed by systematic variation of ligands, metals and other groups of substituents in the transition metal complexes [16, 17]. This systematic study led to the development of mononuclear dyes [18] and polynuclear [19] based on metals such as Ru^{II} [20, 21], Os^{II} [22], Pt^{II} [23], Re^I [24], Cu^I [25] the Fe^{II} [26].

For efficient function of DSSC, used dyes must conform to a series of essential requirements of design. They have to form chemical bonds with TiO_2 by a group of “anchor”. This role, as a rule, play groups carboxylic or phosphonic. They provide efficient injection of electrons in the conduction band of TiO_2 and prevent its gradual shift in the electrolyte. To achieve the charge injection on TiO_2 energy level, Lowest Unoccupied Molecular Orbital (LUMO) of the dye should be greater than the energy of the conduction band of TiO_2 , and for regeneration of oxidized dye his energy levels Highest Occupied Molecular Orbital (HOMO) must be lower than the redox energy level.

Another requirement to dye is intense absorption of solar radiation in the visible spectrum or close to IR region, preferably covering a wide range of wavelengths. It is necessary for electron transfer from the dye on TiO_2 conduction band to be faster compared with the time of the dye excited state deactivation.

Family complexes $\{[(4,4'\text{-COOH})_2\text{-bipy}]_2\text{RuX}_2\}$ (bipy = 2,2'-bipyridyl, X = Cl, Br, I, CN, SCN) works well [27] but the most efficient DSSCs demonstrated to date by the Grätzel group are: the N719 (Fig. 3.2), N3 and 'black' dyes (Fig. 3.3).

Today N₃ dye is still widely employed as a reference, the reported efficiency of 10 % could only be slightly improved since then. DSSCs sensitized with terpyridil-Ru^{II} complex so-called "black dye", have a higher short circuit current. The conversion efficiency of 10.4 % (1 cm²) and 11.1 % (0.26 cm²), are the

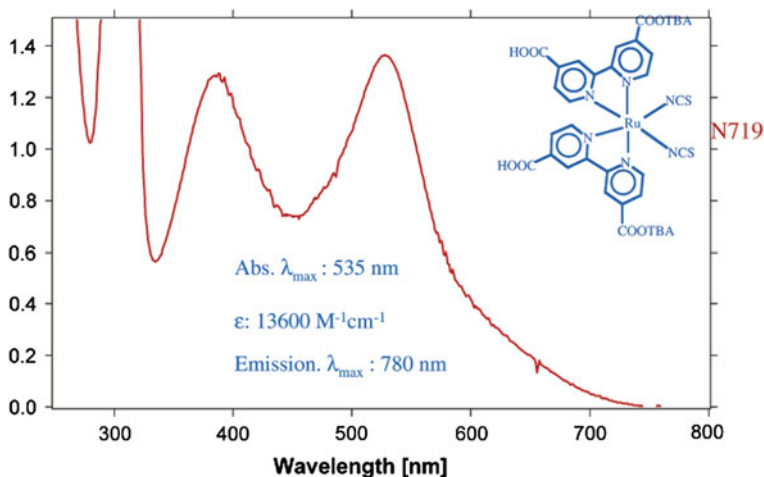


Fig. 3.2 Absorption spectrum of N719 in ethanol. [28]

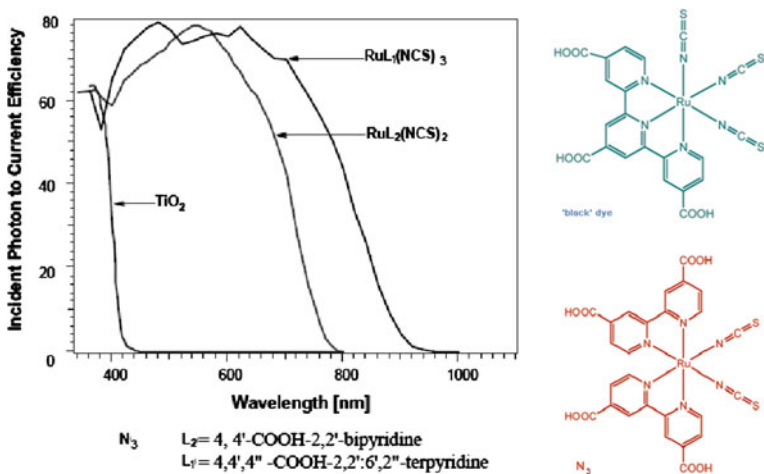
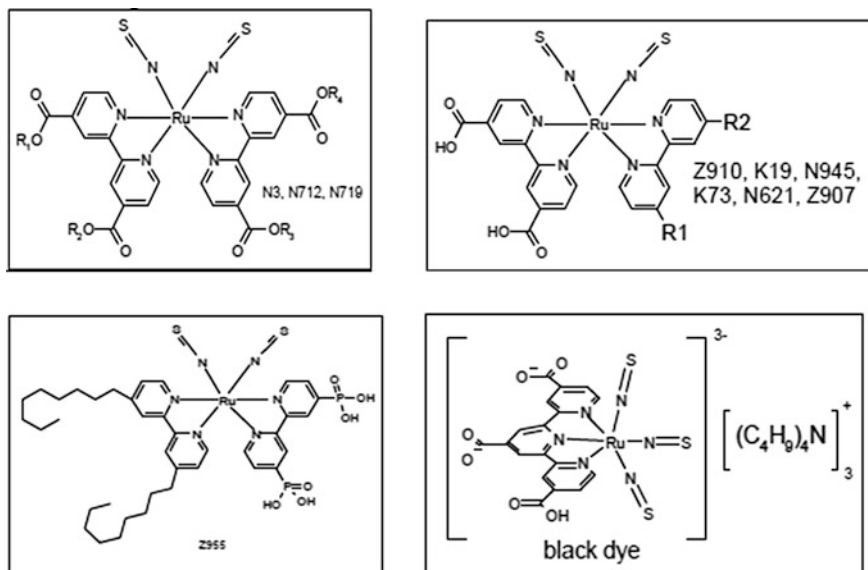


Fig. 3.3 Absorption spectrum of N3 and black dye [29]

highest certified efficiencies so far. However, the stability of the dye has not been proven yet.

Some of good results are achieved with styryl-ligands attached to the bipyridyl ring and presented in Table 3.2. The performance of these novel sensitizers on thick electrodes and with volatile electrolytes is about the same as for the N3-reference (e.g. Z910 10.2 % and N945 10.8 %), but applied on thin electrodes and with non-volatile electrolytes, the conversion efficiency is significantly higher. At the same time a remarkable stability at 80 °C in darkness and at 60 °C under AM1.5 is observed. The excited state of these dyes is between -0.71 and -0.79 V versus NHE, which is sufficiently more negative than the conduction band of TiO_2 (ca. -0.1 V vs. NHE) to ensure complete charge injection [30].



The most remarkably feature about the Ru-dyes is their extraordinary stability when being adsorbed on the TiO_2 -surface. For example, the widely employed complex N3 sustains only 200 excitation cycles in solution, but between 10^7 – 10^8 cycles on a metal oxide surface. The difference between the dye in solution and on the TiO_2 -surface is an ester bond in the periphery of the molecule. Obviously the electronic state of the Ru-complex is significantly altered by the adsorption. The dye is probably not simply attached by physisorption or chemisorption, but creates a charge transfer complex (CTC) with Ti^{3+} -surface states, which are partly present in the semiconductor or are created upon charge injection. The CTC might induce a π -backbonding, which allows the local export of entropy and thus stabilizes the Ru-complex.

3.2.2 Ru(tpy)-Complexes

Sauvage, Balzani and their groups discussed a great number of terpyridine (tpy) derivatives which had been used for preparing of Ru(II) complexes [31]. As can be seen from Table 3.3, ligand substituents cause considerable variations in the absorption and electrochemical properties. It is clear that phenyl substituents in the 4, 4', and 4'' positions increase the molar absorption coefficient, as expected on simple theoretical grounds [32]. The substituent effect on the energy of the absorption and emission bands results from a combined perturbation of the LUMO (ligand π^*) and HOMO (metal t_{2g} , in octahedral symmetry) orbitals. The effect on the luminescence quantum yield and lifetime is likely related to the above-mentioned perturbations as well as to the substituent effect on the ligand field strength. In general, (i) both the electron-withdrawing and donating substituents stabilize the Metal Ligand Charge Transfer (MLCT) excited state, with a consequent red shift on the absorption and emission maxima, and (ii) the electron-withdrawing substituents increase the excited state lifetime and the luminescence intensity at room temperature [31].

The Ru(tpy) $_2^{2+}$ complexes are electrochemically active. They exhibit a reversible Ru^{II,III} oxidation process and a variable number of reversible or quasi-reversible reductive ligand-centered processes. Some of the electrochemical data are presented in Table 3.3. The excited state of all these dyes are more negative than -0.9 V versus NHE, that satisfies condition of complete charge injection in the conduction band of TiO $_2$.

Table 3.3 Photoelectrochemistry characteristics of Ruthenium complexes [31]

Number	Dye	Absorption		Electrochemistry	
		λ (nm)	ϵ ($10^3 \cdot \text{M}^{-1} \text{cm}^{-1}$)	$E_{1/2}$, V	
1.	Ru(tpy) $_2^{2+}$	476	17.7	+1.30	-1.24
2.	Ru(Cl-tpy) $_2^{2+}$	480	16.0	+1.0	-1.53
3.	Ru(Me $_2$ N-tpy) $_2^{2+}$	490	15.4	+0.42	-1.90
4.	Ru(HO-tpy) $_2^{2+}$	485	12.7	+0.73	-1.81
5.	Ru(EtO-tpy) $_2^{2+}$	485	17.5	+0.74	-1.76
6.	Ru(ph-tpy) $_2^{2+}$	488	30.0	+0.90	-1.66
7.	Ru(Cl-phtpy) $_2^{2+}$	490	24.6		
8.	Ru(HO-phtpy) $_2^{2+}$	496	26.1		
9.	Ru(MeO-phtpy) $_2^{2+}$	495	24.4		
10.	Ru(tphtpy) $_2^{2+}$	501	38.4	+1.22	-1.19
11.	Ru(4,4'-dtpy) $_2^{2+}$	495	28.3		
12.	Ru(6,6''-dtpy) $_2^{2+}$	477	6.85		
13.	Ru(ttpy) $_2^{2+}$	490	28.0	+1.25	-1.24
14.	Ru(tppz) $_2^{2+}$	478		+1.51	-0.88
15.	Ru(tpy)(tppz) $_2^{2+}$	470	20.1	+1.50	-0.95
16.	Ru(tpy)(phbp) $^+$	523	9.96	+0.54	
17.	Ru(tpy)(dph) $^+$	550	8.25	+0.49	-1.61

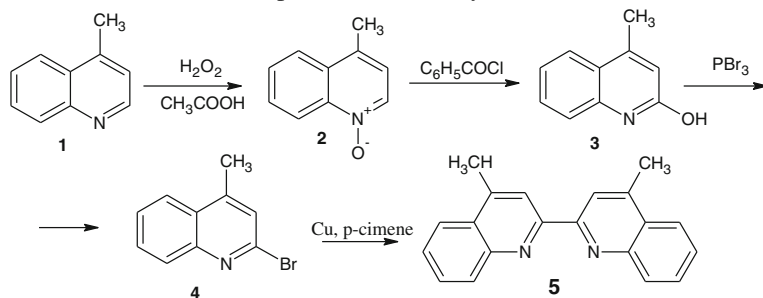
3.3 Synthesis and Characterization of Ligands Based on Bipyridine and Terpyridine (Our Investigations)

3.3.1 Synthesis of 2,2'-Bilepidine Ligand

According to literature, diquinolin complexes have a very high interest to study it in photovoltaic applications [18]. In literature, several methods are noted for the synthesis of 2,2-bipyridinic compounds as ligands, One type of methods was interaction of quinolin with metals in inert gas atmosphere where are obtaining partial hydrogenated isomers of 2,2'-diquinolins, which are oxidized in nitrobenzene and are obtaining diquinolins mix, components of that is depending of metal nature.

In the first method 4-methyl-quinolin was boiled for 8 h with aluminium powder in inert gas atmosphere, activated with HgCl_2 [33]. After separation was obtained 8 different isomers in small amounts, that provoke decreasing of yield of target compound 2,2'-dilepidine (7 %).

Other method of synthesis of ligand could be chosen in a longer pathway. Proceeding of 4-methylquinolin (1) was synthesized 2-bromo-4-methyl-quinoline (4) according to Scheme 1. The synthesis of N-oxylepidine (2) was performed according to the method used by Midjoian [34] with a yield of 55 %. In order to activate the C-2 position of lepidine compound (2) was isomerized and obtained 2-oxilepidine (3), again according to the Midjoian method [35]. The next step of substitution was made according to the Kaslow and Marsh method [36], finally was obtained was 2-brom-lepidine (4) with a yield of 70 %.



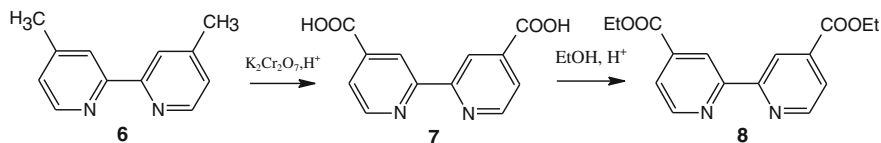
The final step of obtaining 2,2'-bilepidine represents coupling reaction of 2-brom-lepidine with a low active metal, such as Cu. According to the literature that method was also applied to obtain 2,2-bipyridin having a 52–54 % yield [37], but after experience 2,2'-bilepidin was obtained with a yield of 12 % and excessive consumption of the intermediate reactive which motivates to process the proposed methodology in future.

Based on IR and $^1\text{H-NMR}$ spectra, the presence of compounds (1–4) was demonstrated by the appearance and disappearance of characteristic bands. Compound (2) was demonstrated by the appearance of the absorption band of the oximes group $\nu(\text{NO})$ $1,146\text{ cm}^{-1}$, a methyl group $1,395\text{ cm}^{-1}$, and aromatic

groups of quinolin are in $1,300\text{--}1,510\text{ cm}^{-1}$ region. In spectrum of compound (3) disappears absorption band of oximes group and appear --OH group band at $3,190\text{--}3,929\text{ cm}^{-1}$ region. Group --OH from position 2 in lepidine also has been demonstrated by $\text{H}^1\text{-NMR}$ spectroscopy, where the --OH group proton peak observed at 11.28 ppm. Compound (4) was also demonstrated by the disappearance of the absorption band of --OH group and the appearance of $\nu(\text{C--Br})$ bond at $500\text{--}600\text{ cm}^{-1}$, the aromatic methyl group of lepidine was observed in $1,395\text{ cm}^{-1}$ and quinolin rings at $1,300\text{--}1,510\text{ cm}^{-1}$ region. Final compound (5) was demonstrated from $\text{H}^1\text{-RMN}$ spectrum with appearance of singlet of two protons from C3 position, at 7.8 ppm region.

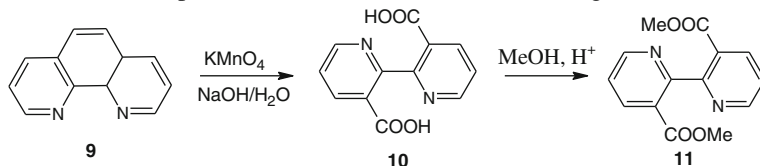
3.3.2 Synthesis of the Ligand 4,4'-Dicarboetoxi-2,2'-Dipyridyl

The aim of this synthesis is the further use of this dye, named N3, as etalon for sensibilisation of titanium oxide (IV) semiconductors. As the starting compound was used 4,4'-dimethyl-2,2'-dipyridyl (6). It was oxidized with potassium dichromate in acid medium according to described method [38]. The reaction was carried out quantitatively (yield 95 %). The obtained 2,2'-dipiridil-4, 4'-dicarboxylic acid (7) was further esterificated in acid solution of ethanol according to described method [39].



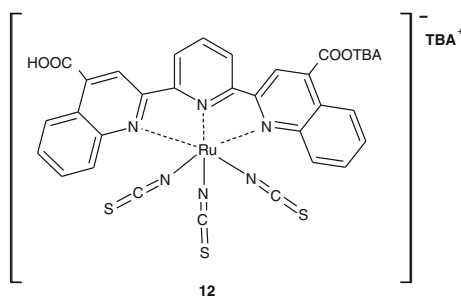
3.3.3 Synthesis of the Ligand 3,3'-Dicarbometoxi-2,2'-Bipyridyl

The bibliographic study [18] showed that is necessary to study new metalorganic chromophore efficient for photovoltaic applications. In order to obtain more accessible ligands was initiated synthesis of compounds 2,2'-dipyridyl-3,3'-disubstituted. The synthesis of acid diethyl ester, 3,3'-dicarbometoxy-2,2'-dipiridil (11) from the 1,10-phenanthroline (9) was done according to the next scheme.



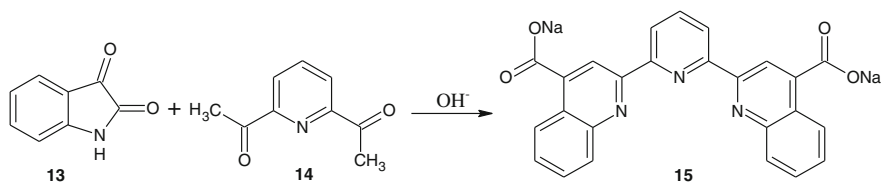
The synthesis of 2,2'-bipyridyl-3,3'-dicarboxylic acid (binicotinic acid) by the oxidation of 1,10-phenanthroline with alkaline permanganate was first described by Smith and Inglett [40]. The preparation of binicotinic acid by this method has subsequently been reported by several workers [41] with yields varying from 50–85 %. We used here the same simplified preparation of binicotinic acid in good yield (65–80 %) with the elimination of the tedious work-up procedure [42]. The esterification method of nicotinic acid was made in methanol and sulphuric acid solution, refluxed, neutralized, separated and dried in vacuum with approximately 50 % yield like in Dholakia procedure [43].

3.3.4 Synthesis of the Ligand 2,6-bis(4-Carboxyquinolin-2-yl)Pyridine



Onozawa-Komatsuzaki report the synthesis and photochemical properties of a new ruthenium complex (12) with a 2,6-bis(4-carboxyquinolin-2-yl)pyridine. This ligand has an extended aromatic structure owing to the existence of two quinoline rings linked with the pyridine ring; therefore, the delocalization and electronegativity of this ligand were expected to lower the energy of the π^* -level and extend the absorption envelope of 12 well into the IR region [44]. This complex exhibited better light-harvesting properties and higher absorbance than those observed for black dye in the near-IR region. DSCs sensitized with 1 showed 35 % Incident-Photon-to-electron Conversion Efficiencies (IPCE) at 900 nm; this is the highest IPCE value reported for ruthenium–polypyridyl complexes in the near-IR region. This demonstrated light-harvesting efficiency makes 12 an attractive candidate as a high-performance sensitizer under near-IR irradiation.

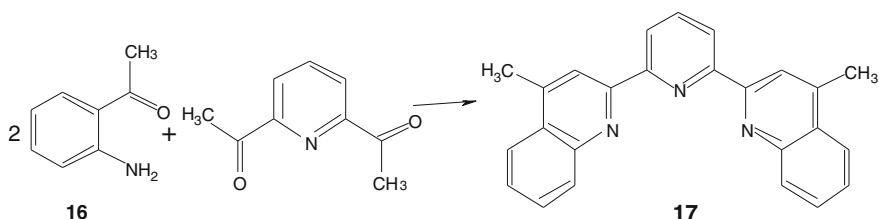
Compound (15) was prepared through a Pfitzinger reaction of isatin (13) and 2,6-diacetylpyridine (14). Simply stirring the reactants in the presence of sodium hydroxide results in the formation of sodium salt (15). As is the case with carboxylate derivatives of related heterocycles, purification of (15) can be troublesome due to its insolubility in all acids, but soluble in bases [45].



C^{13} -NMR was more useful, than proton NMR in the characterization of (15). While the proton NMR contained only aromatic protons the signals were extremely broad and detailed structural information was lacking.

3.3.5 Synthesis of the Ligand 2,6-Bis(4-Methylquinolin-2-yl)Pyridine

The Friedlander condensation is an extremely useful and versatile method for the direct construction of a quinolin ring [46]. The condensation of an aromatic o-aminoaldehyde with an enolizable ketone proceeds directly with the loss of two molecules of water. By varying the nature of the aromatic ring, a variety of annulated quinolines can be prepared. Guiding by this method, at the interaction of o-aminoacetophenone (16) with 2,6-diacetylpyridine was obtained 2,6-bis(4-methylquinolin-2-yl)pyridine.

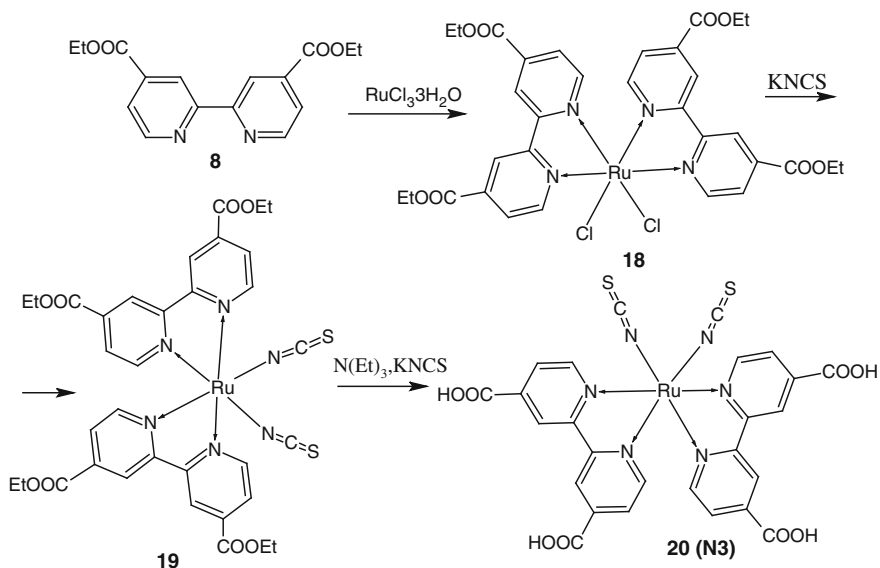


Its structure was demonstrated by IR, C^{13} -NMR, H^1 -NMR, COSY-45 but to say that was formed quinolin ring in 2-C position of pyridine was easily by H^1 -NMR, where was observed a singlet at 8.60 ppm of 2 protons in C^3 position of quinolin rings.

3.4 Complexation of Obtained Ligands

3.4.1 Synthesis of the Etalon-Dye N3

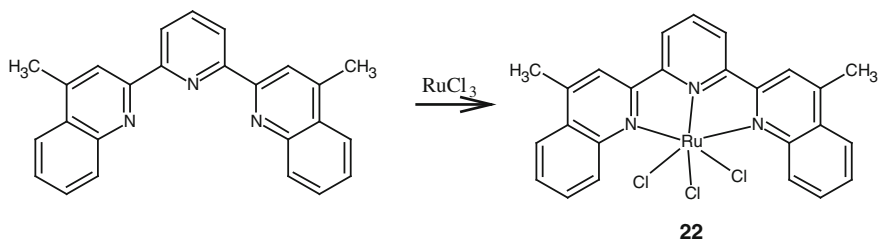
The next scheme shows the stages developed by Grätzel group of researchers [47] for the synthesis of this complex N3. Substances interim and final products were characterized by spectroscopy (^{13}C , 1H) NMR. This compound is very good known in literature and was discussed before.



3.4.2 Complexation of 3,3'-Dicarbomethoxy-2,2'-Bipyridyl

After literature investigation [43, 47] was concluded that complexation methods of 4,4'-disubstituted-2,2'-bipyridyn ligands with Ru^{III} can be applied for complexation of 3,3'-disubstituted-2,2'-bipyridyn ligands. The last step was made in the same procedure described higher (p. 3.4.1).

3.4.3 Complexation of the Ligand 2,6-Bis(4-Methylquinolin-2-yl)pyridine



Ligand 2,6-bis(4-methylquinolin-2-yl)pyridine was complexed with $\text{Ru}(\text{III})$ and was observed that it has peak in visible region of spectrum at 530 nm, which can be used in photocatalytical water splitting processes (Fig. 3.4).

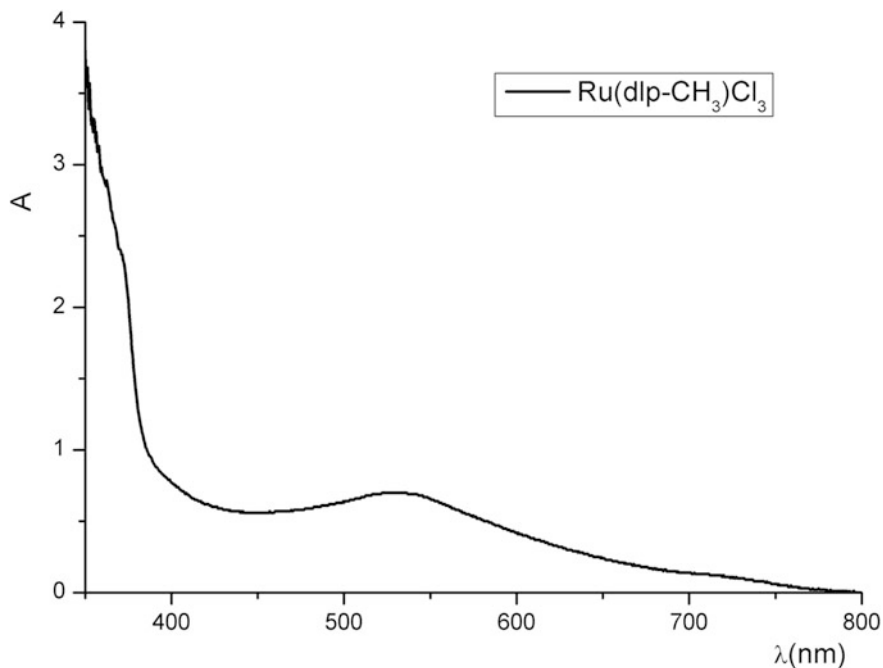
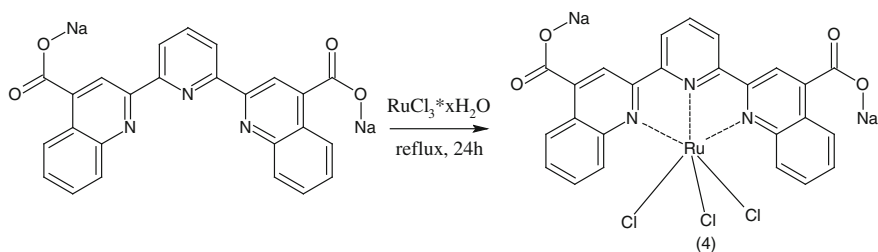


Fig. 3.4 Absorption spectrum of $\text{Ru}(\text{dqp-CH}_3)\text{Cl}_3$ complex (22)

3.4.4 Synthesis of the Complex Disodium-2,6-Bis(4-Carboxylat-Quinolin)Pyridinat of Ruthenium (III)



After refluxation of ligand 2,6-bis(4-carboxyquinolin-2-yl)pyridine (15) with ruthenium chloride it is obtained complex disodium-2,6-bis(4-carboxylat-quinolin)pyridinat ruthenat (III) ($\text{Ru}(\text{dqp})\text{COONa}$) (23). From UV-Vis spectrum it is observed an large absorption peak (690 nm) in UV and visible region (Fig. 3.5).

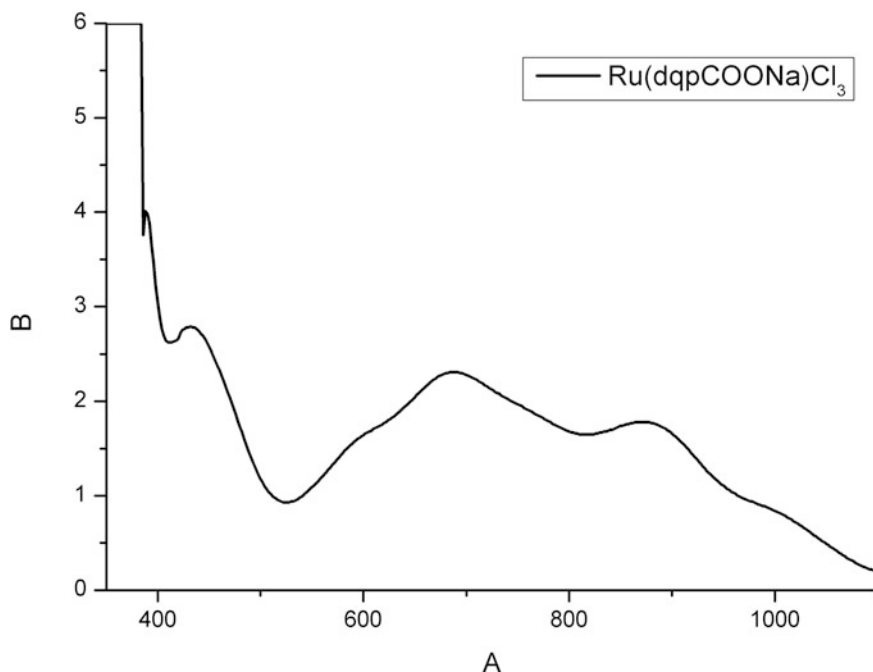


Fig. 3.5 Absorption spectrum of $\text{Ru}(\text{dqp-COONa})\text{Cl}_3$ complex

3.5 Metallo-Phorphirins Complexes

The use of porphyrins as light harvesters in various solar cells is quite reasonable because of an intense absorption in the Q band at low energy as well as in the Soret band at higher energy. On the other hand, numerous attempts to use porphyrins in conversion of solar energy into chemical or electrical energy represent an attempt to mimic the photosynthetic systems found in plants and some bacteria. Chlorophylls (Chls)—the extremely important molecules in natural photosynthesis which absorb light and transfer that light energy by resonance energy transfer in the Photosystems I and II, are compounds based on the modified chlorine macrocycle (dihydroporphyrin) (Fig. 3.6).

In 1993 it was firstly described [48] $\text{Chl-}a/\text{TiO}_2$ couple in a DSSC. Using chlorophyll *a* and compounds obtained by its chemical modification (pheophorbide *a*, Mg-chlorin e_6 , H_2 -chlorin e_6 , Cu-chlorin e_6 and Cu-2- α -Oxymesoisochlorin e_4) IPCE of up to 70 % were obtained. Maximum overall energy conversion efficiency of 2.6 % (under simulated sunlight illumination) was obtained for chlorophyll *a*.

Using a derivative of chlorophyll *a* (Fig. 3.7) another group [49] has obtained an improved overall energy conversion efficiency of 3.1 %. By adding carotenoids as a conjugated spacer they achieved optimization of the overall energy conversion efficiency up to 4.2 % [50].

Fig. 3.6 Structure of chlorophyll a [48]

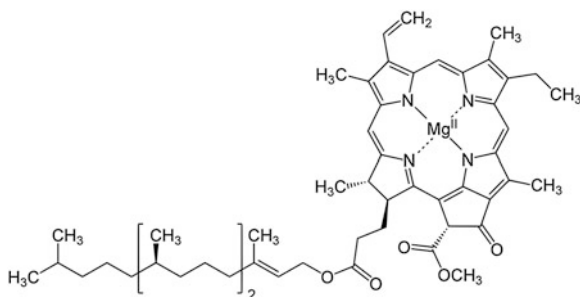
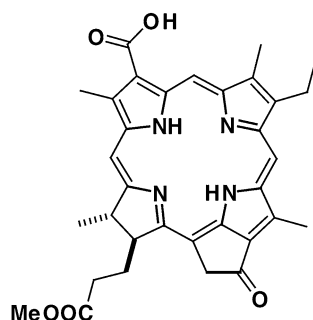


Fig. 3.7 Methyl 3-carboxy-3-devinyl pyropheophorbide a [49]



The influence of carotenoid moiety was investigated by the same group [51]. The authors concluded that introduction of carotenoid moiety to the pheophorbide molecule may result in an electron transfer and singlet-energy transfer from the carotenoid to the chlorin moiety and suppression of the singlet–triplet annihilation reaction. As a result the performance of the cell was enhanced from 1.4 to 1.8 %.

The maximum overall energy conversion efficiency (η) was further improved to 6.5 % by extension of π -conjugation length along the Q_y axis (Fig. 3.8) [52]. This improvement can be explained by two factors: (1) concentration of the electron density in the Q_y direction on the LUMO + 2 for electron injection and (2) better Q_y absorption together with a smaller E_{ox} value for light-harvesting.

Using the knowledge accumulated during the last years a series of new chlorin based compounds was obtained (Fig. 3.9) [53].

The overall energy conversion efficiencies for all DSSCs sensitized with chlorin based dyes exceed 6 % and reach 8 % for dodecyl trans-3²-carboxypyropheophorbide *a* (**3**, Fig. 3.9). This is the highest η value among chlorophyll and porphyrin sensitizers published to date.

Another approach to the cyclic tetrapyrrole molecules for DSSCs sensitizing is the obtaining of synthetic porphyrins. The porphyrin sensitizer with the highest overall energy conversion efficiency ($\eta = 3.0$ %) until 2004 was tetra(4-carboxyphenyl)porphyrin (Fig. 3.10) [54]. The relatively low η value of the sensitizer was explained by the highly symmetrical structure and aggregation of porphyrin molecules.

Fig. 3.8 Methyl trans-32-carboxypyropheophorbide a and its LUMO + 2 molecular orbital [52]

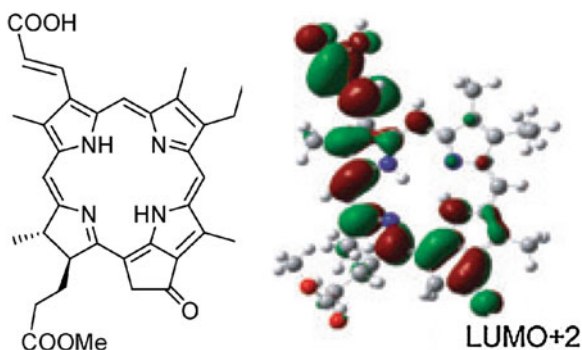


Fig. 3.9 Chemical structures of chlorin based sensitizers [53]

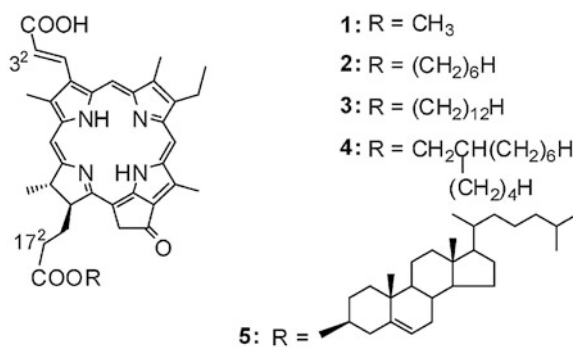
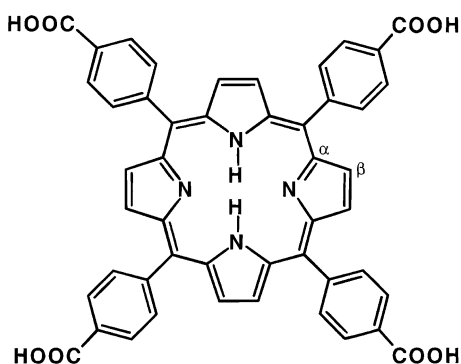


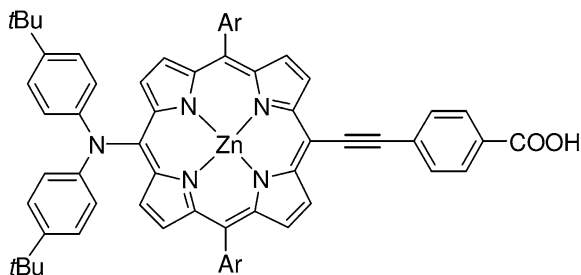
Fig. 3.10 Structure of tetra(4-carboxyphenyl)porphyrin [54]



By unsymmetrical π -elongation of the porphyrin and connection of the linker moiety to the β -position of the porphyrin the Japanese researchers [55] designed a naphthyl-fused zinc porphyrin with a conversion efficiency of 4.1 % (50 % higher comparatively to the unfused porphyrin reference).

In a more recent paper researchers from Taiwan synthesized a *meso*-substituted porphyrin sensitizer with Donor- π -Acceptor configuration (Fig. 3.11) [56].

Fig. 3.11 Zinc(II) 5,15-Bis(3,5-di-tert-butylphenyl)-10-(bis(4-tert-butylphenyl)amino)-20-(4-carboxyphenylethynyl)porphyrin [56]



This molecule shows very high η value of up to 6.0 % under standard global AM 1.5 solar conditions, which is similar to *cis*-Ru(dcbpy)₂(NCS)₂ dye (**N3**) under the same experimental conditions. It clearly shows that porphyrins can compete with traditional Ru-porphyrin dyes.

Many groups have studied the influence of donor and acceptor moieties on the photosensing properties of sensitizing dyes. Hiroshi Imahori, Shunichi Fukuzumi and co-workers have obtained molecular photovoltaic devices with the porphyrins and fullerenes as the main building blocks [57]. Fullerenes is an electron acceptor with small reorganization energies during the electron-transfer reduction. The porphyrin-fullerene dyads with sulfur-containing group were adsorbed on the gold surface. As a result the charge separated state is formed (Fig. 3.12) and the photocurrent is generated.

The photocurrent intensity in Au/2/MV²⁺/Pt device was enhanced fivefold compared to that in the porphyrin device without C₆₀. This clearly shows that introduction of donor group in the photosensitizer may be useful for optimization of photosynthetic systems mimicking nature. These dyads were extended to ferrocene (Fc)-porphyrin (P)-fullerene (C₆₀) triads (Fig. 3.12).

The introduction of ferrocene group leads to Fc⁺-P-C₆₀—charge-separated state as a result of photoinduced electron transfer (Fig. 3.13). The internal quantum yields of the photocurrent generation for these systems are one of the highest for the donor–acceptor linked molecules at monolayer-modified metal electrodes and in artificial membranes.

The same group has developed photosynthetic system based on boron-dipyrrin (bodipy) and Fc-porphyrin-C₆₀ triad (Fig. 3.14) [58]. The boron dipyrin thiol was chosen as a light-harvesting molecule (λ_{\max} 500 nm, $\epsilon \sim 10^5 \text{ M}^{-1} \text{ cm}^{-1}$) which enhance the absorption of light in green and blue region. The mixed dyes were tuned so that bodipy emission (~ 510 nm) overlaps with the absorption of the porphyrin Q bands (500–700 nm) and an efficient singlet–singlet energy transfer from bodipy moiety to the porphyrin moiety leads to efficient photocurrent generation. But, in these systems the porphyrin excited state is strongly quenched by the gold surface. That is why gold surface was replaced by indium tin oxide (ITO) and as a result the electron injection from P* to fullerene was achieved, without quenching by the ITO surface. The internal quantum yields obtained by Hiroshi Imahori and Shunichi Fukuzumi group reach 50 %, however the power-conversion

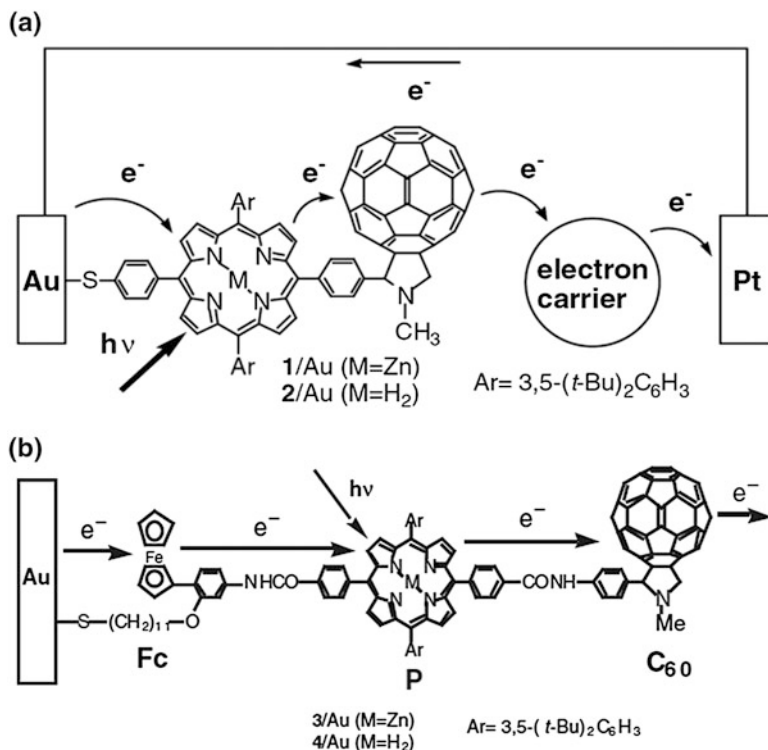


Fig. 3.12 a Photoinduced electron transfer at gold electrodes modified with self-assembled monolayers of porphyrin-C60 dyads [57] b Photoinduced electron transfer at gold electrodes modified with self-assembled monolayers of Fc-porphyrin-C60 [57]

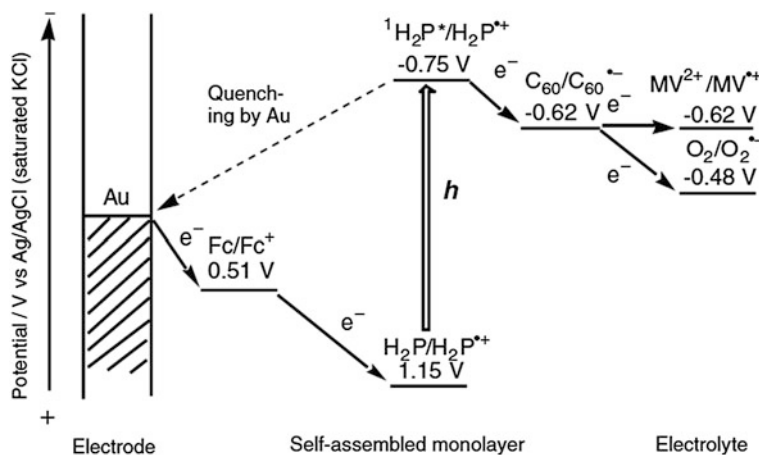


Fig. 3.13 Photoinduced electron transfer at gold electrodes modified with self-assembled monolayers of Fc-porphyrin-C60 alkanethiols [57]

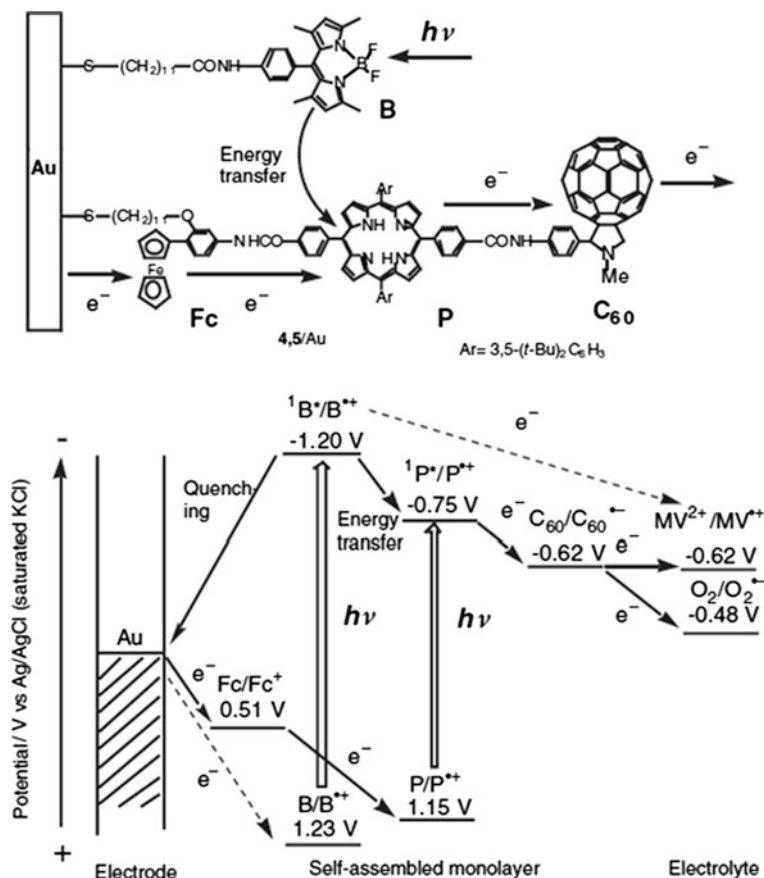
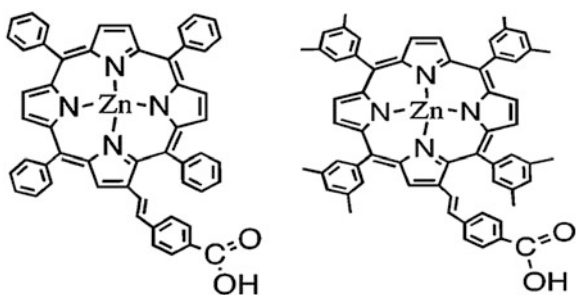


Fig. 3.14 Photoinduced energy transfer and at gold electrodes modified with mixed self-assembled monolayers of ferrocene-porphyrin-C60 alkanethiol and boron dipyrin thiol [58]

efficiency of these systems ($\sim 1\%$) is still lower than that of typical inorganic solar cells.

Another approach for design of synthetic porphyrin based dyes is introduction of anchoring, π -extending moieties at the β -positions. The Officer and coworkers have designed a series of β -substituted porphyrins for sensitization of TiO_2 surfaces [59]. The Cu porphyrins and those with phosphonic acid as anchoring group showed low η values, but the Zn porphyrins with β -substituted ethenylbenzoic acid as anchoring moiety (Fig. 3.15) give high overall energy conversion efficiency of up to 4.8%. It is to be emphasized that the introduction of *m*-methyl substituents on the *meso*-phenyl groups give rise with 16% of η value (4.11 \rightarrow 4.8%), probably by preventing π - π stacking between porphyrin molecules.

Fig. 3.15 Zn porphyrins with β -substituted ethynylbenzoic acid as anchoring moiety [59]



In the [60] is described synthesis of a series of porphyrins β -substituted with carboxylate anchoring groups (Fig. 3.16) for sensitization of nanocrystalline TiO_2 films.

The Incident Photon to electron Conversion Efficiencies (IPCE) of the obtained porphyrins reach 85 % (Fig. 3.17). Among the reported porphyrins, the porphyrin **1** shows the best conversion efficiency of 5.2 % under standard AM 1.5 sunlight. By analyzing obtained results can be revealed the influence of the anchoring group on the photovoltaic properties of the photosensitizer.

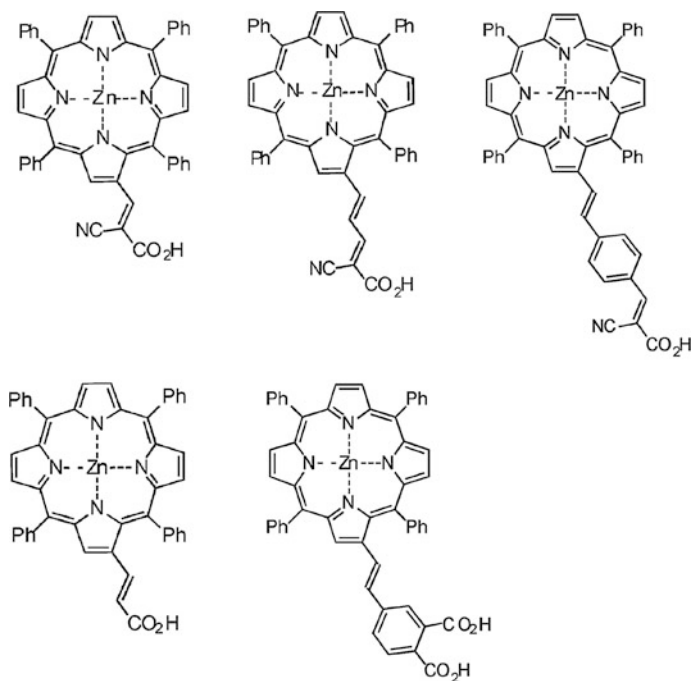


Fig. 3.16 β -Modified porphyrins 1–5 [60]

Fig. 3.17 Photoaction spectra of porphyrins 1–5 [60]

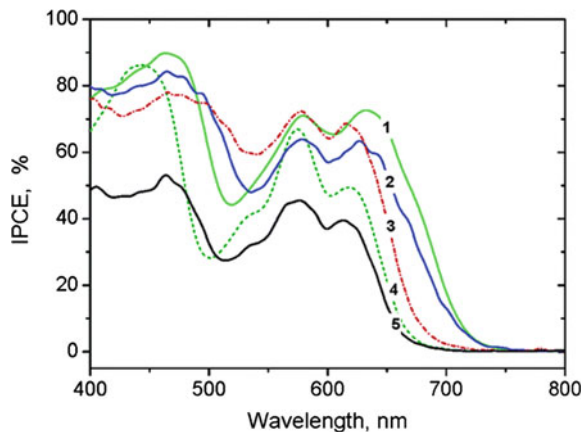
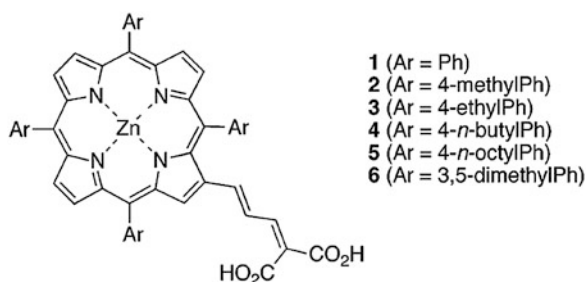


Fig. 3.18 β -Modified porphyrins 1–6 [61]

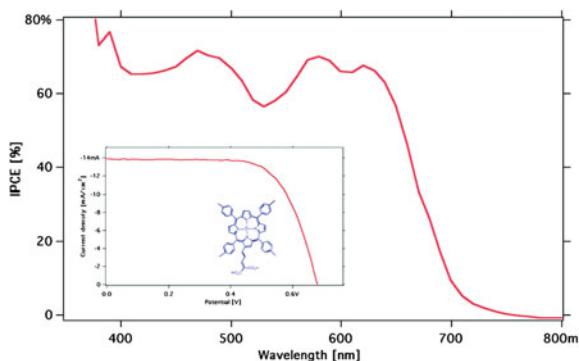


In the following work [61] the same group has changed the aryl substituent in *meso*-position of porphyrins (Fig. 3.18) to determine its influence on the IPCE of the dyes.

The porphyrin 2 of this set shows high IPCE values (Fig. 3.19) and the overall conversion efficiency of 7.1 % (3.6 % for solid state cell) under standard global AM 1.5 solar conditions, which is the best η value among the present and reported synthetic porphyrin sensitizers for DSSCs. However, all of the dyes 1–6 exhibit efficiencies ≥ 5 %. It is indicating that the nature of the substituents of the aryl group is not a major factor in determining photosensing properties of dyes.

Conclusion: Porphyrins of different metals with substituents in *meso* and β -pyrrole positions are the perspective dyes for DSSC devices.

Fig. 3.19 Photoaction spectrum of porphyrin 2 [61]



3.6 Synthesis and Characterization of Tetra (Ferrocene) Porphyrins (Our Investigations)

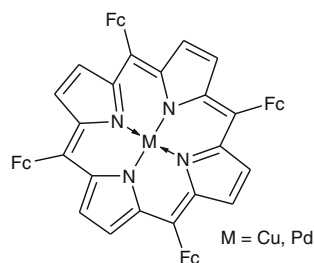
Pd and Cu tetra(ferrocenyl) porphyrins were obtained in our laboratory (Fig. 3.20). Their UV-Vis spectra (Fig. 3.21) show very high absorption in the entire visible region of light. A new band ($\lambda_{\text{max}} = 475, 480$ and 486 nm for free-metal, Pd (II) and Cu (II) tetra(ferrocenyl) porphyrins, respectively) appeared in comparison with tetra(phenyl) porphyrins.

As a result these porphyrins show high harvesting properties for 300–700 nm spectrum of light.

The Cyclic voltammetry (CV) spectra (Fig. 3.22) of the synthesized porphyrins show reversible processes in the potential window -2 to $+1$ V in THF and DMF vs Ag/AgCl.

Two reversible peaks in the negative (reductive) potential region were attributed to the one electron reductions of the porphyrin ring. The quasireversible peak in the positive (oxidative) potential region was attributed to the oxidation of the four ferrocenyl moieties. The reduction of the obtained ferricinium moieties shows a wave with a very large area which was attributed to the desorption processes of the positively charged species deposited on the electrode surface.

Fig. 3.20 Tetra(ferrocenyl)-porphyrine of Cu and Pd



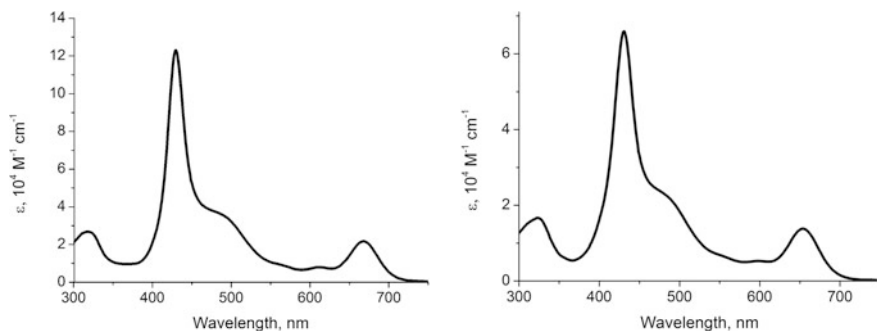


Fig. 3.21 The UV-Vis spectra of tetra (ferrocenyl)-porphyrine of Cu (*left*) and Pd (*right*) in THF

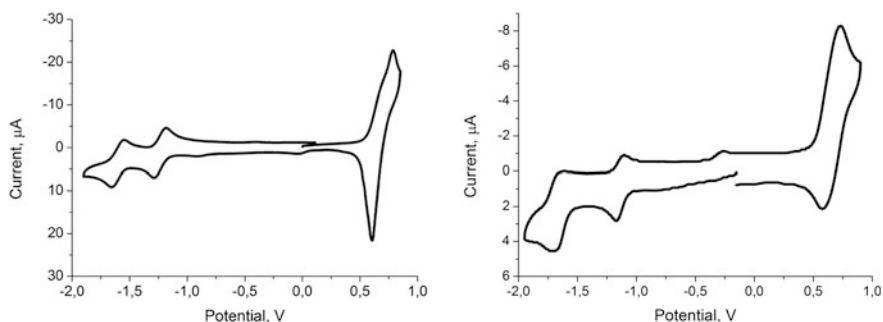


Fig. 3.22 CV spectra of Cu tetra (ferrocenyl) porphyrin in THF and Pd tetra (ferrocenyl) porphyrin in DMF (0.2 M TBATFB) at a glassy carbon working electrode. Scan rate = 100 mV s^{-1}

The obtained results indicate that meso-ferrocenyl porphyrins have potential to be used as molecular sensitizers for harvesting the sunlight.

References

1. Richard C Willson, Hugh S Hudson (1991) *Nature* 351:42–44
2. National Renewable Energy Laboratory (NREL). <http://www.nrel.gov/pv/>
3. Energy Inform Administration (2010) Annual energy outlook 2011, December 2010. DOE/EIA-0383
4. Fujishima A, Honda K (1972) *Nature* 238:37
5. Luzzi A (ed) (2004) Photoelectrolytic production of hydrogen, Final report of annex 14, International energy agency, hydrogen implementing agreement (www.ieahia.org)
6. Grätzel M (2001) *Nature* 414:338
7. Bandara J, Weerasinghe HC (2004) *Sri Lankan J Phys* 5:27–35
8. Gurney RW, Mott N (1938) *Proc R Soc A* 164:151
9. Gerischer H, Tributsch H (1968) *Ber Bunsenges Phys Chem* 72:437
10. Memming R (1972) *Photochem Photobiol* 16:325

11. Spitler M, Calvin MJ (1977) *Phys Chem* 67:5193
12. Tsubomura H, Matsumura M, Nomura Y, Amamia T (1979) *Nature* 261:402
13. Regan BO, Grätzel M (1991) *Nature* 353:737
14. Vlachopoulos N, Liska P, Augustynski J, Gratzel MJ (1988) *Am Chem Soc* 110:1216
15. Gratzel M, Kalayanasundaram K (1994) *Current Sci* 66:706
16. Nazeeruddin MK, Grätzel M (2004) In: McCleverty JA, Meyer TJ (eds) *Comprehensive coordination chemistry II*, 9:719–758
17. Argazzi R, Iha NYM, Zabri H, Odobel F, Bigozzi CA (2004) *Coord Chem Rev* 248:1299
18. Nazeeruddin MK, Gratzel M (2007) *Struct Bond* 123:113–175
19. Bigozzi CA, Argazzi R, Kleverlaan CJ (2000) *Chem Soc Rev* 29:87
20. Nazeeruddin MK, Kay A, Rodicio I, Humphry-Baker R, MTTler E, Liska P, Vlachopoulos N, Grätzel M (1993) *J Am Chem Soc* 115:6382
21. Nazeeruddin MK, Pechy P, Grätzel M (1997) *Chem Commun* 18:1705
22. Grätzel M (2003) *J Photochem Photobiol, C* 4:145
23. Geary EAM, Yellowlees LJ, Jack LA, Oswald IDH, Parsons S, Hirata N, Durrant JR, Robertson N (2005) *Inorg Chem* 44:242
24. Hasselmann GM, Meyer GJ (1999) *Z Phys Chem* 212:39
25. Alonso-Vante N, Nierengarten J-F, Sauvage J-P (1994) *J Chem Soc Dalton Trans* 11:1649
26. Jayaweera PM, Palayangoda SS, Tennakone K (2001) *J Photochem Photobiol, A* 140:173
27. Nazeeruddin MK, Kay A, Rodicio I, Humphry-Baker R, MTTler E, Liska P, Vlachopoulos N, Grätzel M (1993) *J Am Chem Soc* 115:6382–6390
28. Gratzel M (2005) *Inorg Chem* 44:6841–6851
29. Gratzel M (2003) *J Photochem Photobiolog C: Photochem Rev* 4(2):145–153
30. http://www.diss.fu-berlin.de/diss/servlets/MCRFileNodeServlet/FUDISS_derivate_000000002568/02_2.pdf?hosts=
31. Sauvage J, Baltani V (1994) *Chem Rev* 94:993–1019
32. Phifer CC, McMillin DR (1986) *Znorg Chem* 25:1329
33. Sheikman A, Calafat V (1997) *Chemistry of Heterocyclic compounds* 3:385–390
34. Midjoian OL, Shteiman BI (1960) *Synthesis of heterocyclic compounds* 5:37. Publisher Armenia SSR, Erevan
35. Midjoian OL (1960) *Synthesis of heterocyclic compounds* 5:39. Publisher Armenia SSR, Erevan
36. Kaslow CE, Marsh MM (1947) *JOCEAH J Org Chem* 12:456,457
37. Midjoian OL (1969) *Synthesis of heterocyclic compounds* 8:25. Publisher Armenia SSR, Erevan
38. Oki AR, Morgan RJ (1995) *Synth Commun* 25(24):4093–4097
39. Ciana LD, Dressick WJ, Zelewsky A (1990) *J Heterocyclic Chem* 27:163
40. Inglett GE, Smith GF (1950) *J Am Chem Soc* 72:842
41. Echard IF, Summers LA (1973) *Australian J Chem* 26:2727
42. Wimmer FL, Wimmer S (1983) *OPPI BRIEFS* 15(5):367–368
43. Dholakia S, Gillard R, Wimmer F (1985) *Polyhedron* 4(5):791–795
44. Onozawa-Komatsuzaki N, Sugihara H (2009) *Inorg Chem Comm* 12:1212–1215
45. Bass Y, Morgan RJ (1997) *Synth Commun* 27:2165
46. Thummel RP (1992) *Synlett* 1992:1
47. Shklover V, Nazeeruddin M, Zakeeruddin S, Gratzel M (1997) *Chem Mater* 9:430–439
48. Kay A, Grätzel M (1993) *J Phys Chem* 97:6272
49. Wang X-F, Xiang J, Wang P, Koyama Y, Yanagida S, Wada Y, Hamada K, Sasaki S, Tamiaki H (2005) *Chem Phys Lett* 408:409
50. Wang X-F, Matsuda A, Koyama Y, Nagae H, Sasaki S, Tamiaki H, Wada Y (2006) *Chem Phys Lett* 423:470
51. Wang X-F, Koyama Y, Wada Y, Sasaki S, Tamiaki H (2007) *Chem Phys Lett* 439:115
52. Wang X-F, Kitao O, Zhou H, Tamiaki H, Sasaki S (2009) *Chem Commun* 2009:1523
53. Wang X-F, Tamiaki H, Wang L, Tamai N, Kitao O, Zhou H, Sasaki S (2010) *Langmuir* 26(9):6320

54. Cherian S, Wamser CC (2000) *J Phys Chem B* 104:3624
55. Tanaka M, Hayashi S, Eu S, Umeyama T, Matano Y, Imahori H (2007) *Chem Commun* 2007:2069
56. Lee C-W, Lu H-P, Lan C-M, Huang Y-L, Liang Y-R, Yen W-N, Liu Y-C, Lin Y-S, Diau EW-G, Yeh C-Y (2009) *Chem-Eur J* 15:1403
57. Imahori H, Fukuzumi S (2004) *Adv Funct Mater* 14(6):525
58. Hasobe T, Imahori H, Kamat PV, Ahn TK, Kim SK, Kim D, Fujimoto A, Hirakawa T, Fukuzumi S (2005) *J Am Chem Soc* 127:1216
59. Nazeeruddin MK, Humphry-Baker R, Officer DL, Campbell WM, Burrell AK, Grätzel M (2004) *Langmuir* 20:6514
60. Wang Q, Campbell WM, Bonfantani EE, Jolley KW, Officer DL, Walsh PJ, Gordon K, Humphry-Baker R, Nazeeruddin MK, Grätzel M (2005) *J Phys Chem B* 109:15397
61. Grätzel M, David L (2007) *Officer. J Phys Chem C* 111(32):11760–11762